ISSN 1023-1935, Russian Journal of Electrochemistry, 2021, Vol. 57, No. 12, pp. 1157–1163. © Pleiades Publishing, Ltd., 2021.
Russian Text © The Author(s), 2021, published in Elektrokhimiya, 2021, Vol. 57, No. 12, pp. 762–768.

Synthesizing Zinc Sulfide Films on the Gold Surface as the Sensor for Electrochemical Quartz Crystal Microbalance

D. O. Krinitsyn[a, b, *], A. S. Romanchenko[a, **], S. A. Vorob'ev[a], M. N. Likhatskii[a], A. A. Karacharov[a], A. S. Krylov[c], M. N. Volochaev[c], and Yu. L. Mikhlin[a]

[a] *Institute of Chemistry and Chemical Technology, Siberian Branch, Russian Academy of Science, Krasnoyarsk, Russia*
[b] *Siberian Federal University, Krasnoyarsk, Russia*
[c] *Kirenskii Institute of Physics, Siberian Branch, Russian Academy of Science, Krasnoyarsk, Russia*
**e-mail: dok14@mail.ru*
***e-mail: romaas82@mail.ru*

Received December 15, 2020; revised March 19, 2021; accepted April 13, 2021

Abstract—A zinc sulfate film is deposited from aqueous solutions of zinc sulfate onto the gold surface with the aim of preparation of a sensor for electrochemical quartz crystal microbalance (EQCM). The kinetics of this process, the particles formed in solution, and the film itself are studied by the methods of electrochemical quartz crystal microbalance, X-ray photoelectron spectroscopy, transmission electron microscopy, atomic force microscopy, optical and Raman spectroscopies, and dynamic light scattering. The effect of the procedure of gold surface preparation, the reagent concentration, and the temperature on the film adhesion, the length of induction period, the kinetics of film growth, and its structure and thickness are studied. It is shown that the film formation proceeds as a result of deposition of sufficiently coarse 200–700 nm colloid particles of sphalerite. It is demonstrated that this sensor can be used in studying the electrochemical reactions of ZnS and the interface phenomena by the methods of EQCM and cyclic voltammetry.

Keywords: sphalerite, thin films, hydrochemical deposition, electrochemistry, quartz crystal microbalance, dynamic light scattering, gold, spectroscopy

DOI: 10.1134/S1023193521120041

INTRODUCTION

Sphalerite ZnS is the main mineral and the natural source of zinc and also the most important material for optoelectronics and solar cells, semiconducting engineering, sensors, and other applications [1–4]. This is why the attention of scientists is focused on studying the surface phenomena and electrochemical reactions of zinc sulfide [5]. The electrochemical quartz crystal microbalance (EQCM), is a very sensitive technique which allows studying the electrochemical behavior and properties of interfaces, for example, the hydrophobic properties of surfaces. Sphalerite is a wide energy-gap semisonductor with the band gap of 3.54–3.91 eV [6]; due to its low conductivity, its electrochemical studies were few and carried out with the use of, e.g., paste electrodes [7, 8]. In the EQCM technique, the material is deposited onto the sensor as a thin film, which is not a trivial task for sulfide materials. The sensors for EQCM measurements are usually produced by multi-layered deposition onto AT quartz where the outer layer is gold, platinum, or any other material and the intermediate layers are the sputtered chromium or titanium films. The company Biolin Scientific produces Q-sense sensors with the outer layer of zinc sulfide deposited from the gas phase onto the titanium sublayer. However, it is difficult to use these sensors in aggressive media, experiments with polarization, and, especially, use them repeatedly [9]. Probably, due to the difficulties in the preparation of sensors with the outer sulfide coating, the EQCM studies on metal sulfides are so scarce.

On the other hand, several methods were proposed for preparation of ZnS films, which include chemical deposition from the gas phase, molecular beam epitaxy [10–12], and chemical deposition from aqueous solutions [10–12]. The methods of the latter group are the simplest, because the process can be carried out at low temperature (from 25 to 100°C) with the use of simple equipment and available reagents and also onto brittle, chemically and thermally unstable supports. The literature contains several references in which the methods of deposition of zinc sulfide on different supports (optically transparent glass, Au, CdS, $GaInS_2$, etc.) are described and the factors determining the characteristics of produced films are discussed [10–15]. Nonetheless, many problems still remain open, including the mechanism of hydrochemical deposition.

This study is aimed at the development of a sensor based on zinc sulfate for measurements by the method of electrochemical quartz crystal microbalance. For this purpose, it was necessary to develop a simple method for deposition of the zinc sulfide film (preferentially sphalerite) onto the gold coating of a QCM sensor and to demonstrate the efficiency of the latter.

EXPERIMENTAL

As the supports, we took 5 MHz sensors for quartz crystal microbalance (Phillip Technologies, USA) with the gold-electrode surface area of 1 cm^2 which were compatible with QCM 200 (Stanford Research Systems, USA). As the sulfidizing agent we used thiourea. The solution for deposition contained zinc sulfate and Trilon-B, its pH was regulated by adding concentrated NaOH solution. For solutions, we used reagents with the purity grade not lower than the reagent grade and also deionized water. The 200 mL reaction vessel was controlled at the temperature of 60–85°C. In a typical experiment, after the working temperature was established, 5 mL deionized water, 20 mL EDTA, 2.5 mL 0.1 M zinc sulfate, 50 mL 2 M NaOH were added to the vessel on stirring with a magnetic stirrer. 20 mL of 1 M solution of thiourea was added to the bath immediately before measuring the QCM signal.

The sensors were pretreated in order to activate their surface and increase the adhesion of zinc sulfide. The typical process involved 10 min treatment in 50 mL acetone in a supersonic bath and washing with a large amount of water. The gold surface was etched in the piranha solution (1 vol 33% H_2O_2 + 3 vol 98% H_2SO_4) or another reagent (2 M nitric acid, 1 M sulfuric acid, sodium sulfide solution, or NaOH solution), thoroughly washed with water in supersonic bath, and dried in air.

Electrochemical studies were carried out by a QCM 200 device and a potentiostat EC 301 (Stanford Research System, USA). As the counter electrode, we used a platinum wire. The potential was measured with respect to a saturated silver chloride electrode; all potentials are related to this electrode. As the working electrode solution we used 0.05 M sodium tetraborate. The potential scan rate was 20 mV/s both in anodic and cathodic directions starting from the compromise potential.

The images of the sensor surface were obtained by the atomic force microscopy (AFS) in the semicontact mode by a scanning multimode probe microscope Solver P-47 (NT-MDT, Russia) in air at room temperature. As the probes, we used silicon cantilevers with resonance frequency of 150–250 kHz. X-ray photoelectron spectra (XPS) were measured on SPECS spectrometer with a semispherical energy analyzer PHOIBOS 150 MCD9 on excitation by AlK_α monochromatic radiation from the X-ray tube anode (1486.6 eV) at the electroanalyzer pass energy of 20 eV for overview spectra or 10 eV (narrow scans). The spectra were processed by using software CasaXPS. The ratio of elements on the surface was determined from overview spectra with the use of empirical coefficients of sensitivity. The particle size in the reaction solution was measured by using spectrometer Zetasizer Nano ZS (Malvern Instruments, UK) with the wavelength of laser radiation of 633 nm. The Raman spectra were obtained on spectrometer Horiba Jobin-Yvon T64000 (Horiba, Japan).

RESULTS AND DISCUSSION

Deposition of ZnS Film onto the Surface of Gold Coating Sputtered on a Quartz Sensor

Figure 1a exemplifies the variations in the frequency of an Au-covered sensor depending on the reaction media with different temperature and composition. The initial shift of frequency is associated with the immersion of sensor into solution, after which the frequency remains virtually unchanged for several minutes or hours and then decreases at the slowly decreasing rate, which is associated with the gain in the electrode mass as the zinc sulfide film grows. As expected, the induction period of deposition shortens and the deposition rate increases with the increase in the solution temperature and concentration of zinc ions and also with the increase in the alkali concentration (is not shown). Figure 1b shows the changes in the hydrodynamic size of particles determined by dynamic light scattering (DLS) in samples taken from solution and measured at the same temperature. It is seen that the induction period also takes place, albeit shorter. The dependence passes through the maximum after which the decrease in the particle size can obviously be explained by the loss of aggregative stability of the sol and the deposition of coarser particles. The position of the maximum in time approximately coincides with the end of induction period of film growth on the sensor. Hence, the mechanism of deposition is obviously associated with the deposition of already formed coarse particles onto the gold support rather than with the parallel growth of particles on the sensor surface and in solution.

Figure 2 shows the AFM images of formed films, according to which the size of deposited particles is 200–800 nm, increases with the decrease in temperature, and approximately correlates with the hydrodynamic diameter of particles before the maximums in Fig. 1b, albeit does not coincide completely. For the slower deposition (Fig. 1d), the particle size decreases but the uniformity increases. On the whole, these results agree with the mechanism of film formation by the deposition of coarse particles from solution.

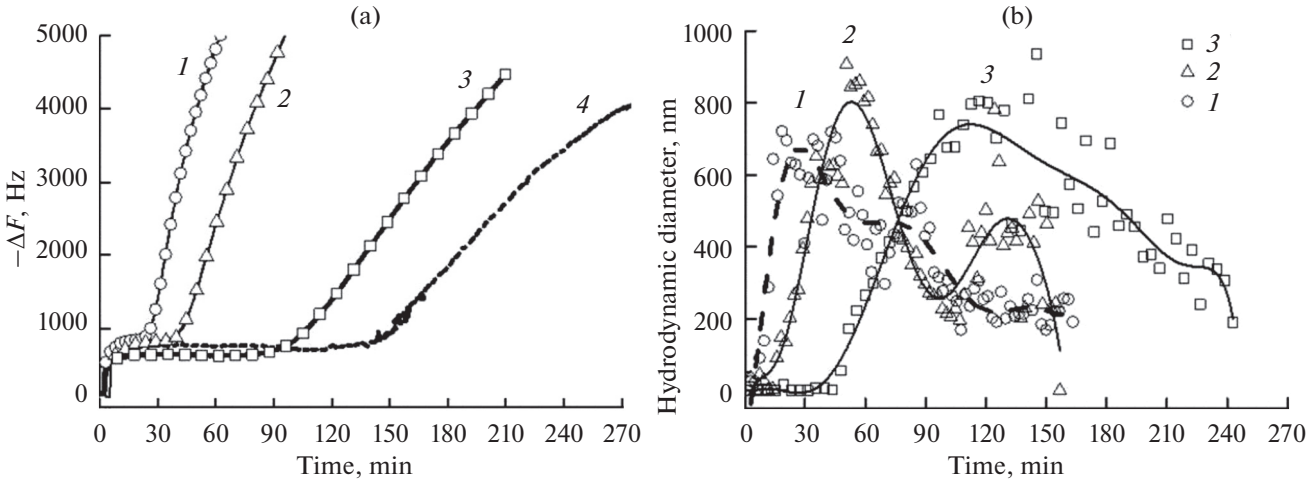

Fig. 1. (a) Changes in the frequency of vibrations of a quartz sensor and (b) the kinetics of changes in the size of particles in solution volume according to DLS data. Experimental conditions: 2.5 mM $ZnSO_4$, temperature, °C: (*1*) 85, (*2*) 75, (*3*) 65; (*4*) 1.0 mM $ZnSO_4$, 65°C (0.04 M Na_2EDTA, 0.2 M thiourea, 1 M NaOH).

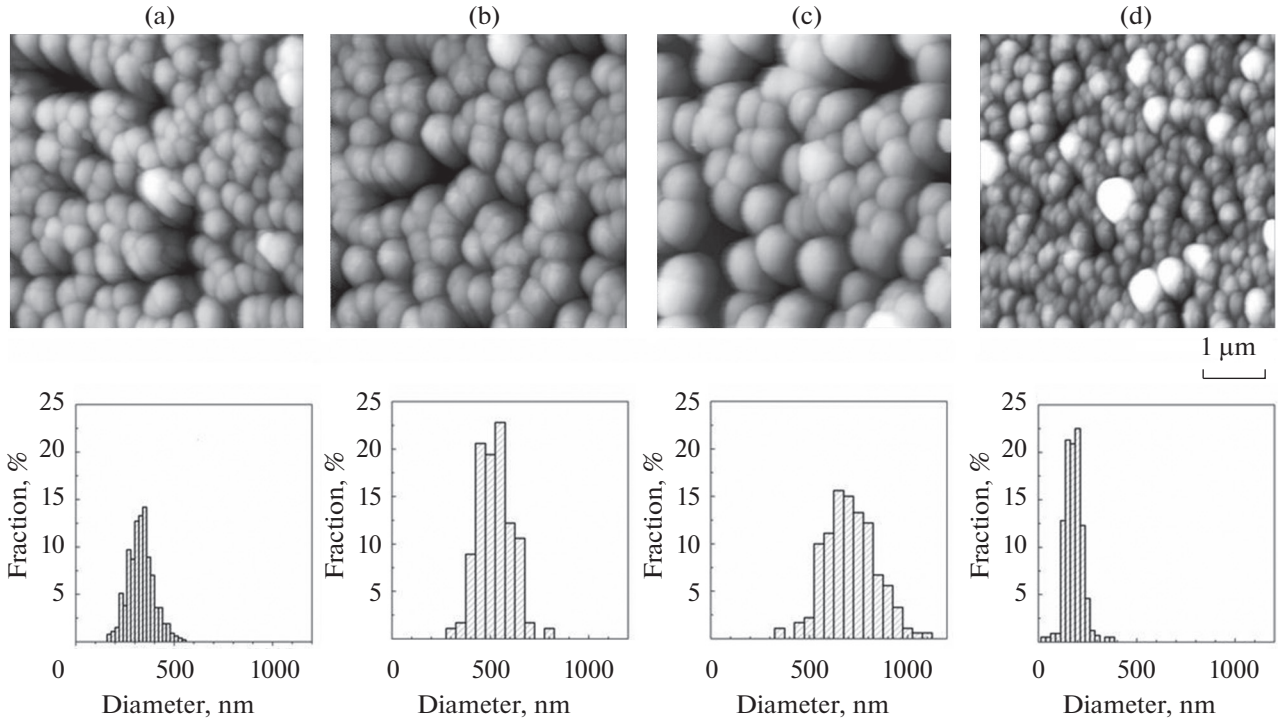

Fig. 2. (top) AFM images of the surface of ZnS film deposited in (a) 2.5 mM $ZnSO_4$, 85°C; (b) 2.5 mM $ZnSO_4$, 75°C; (c) 2.5 mM $ZnSO_4$, 65°C; (d) 65°C, 1.0 mM $ZnSO_4$. (bottom) The corresponding histograms of the size distribution of grains.

As expected, the changes in the frequency dF are directly proportional to the changes in the sensor mass caused by deposition of sulfide on its surface (provided this mass is uniformly distributed as a thin and dense film) [16–19]:

$$dm = udF. \quad (1)$$

Figure 3 shows the TEM image of the cross section of sensor with the ZnS film the deposition of which was accompanied by the decrease in frequency by 6700 Hz. The deposited material demonstrated good adhesion to the gold coating and the dense structure somewhat loosening in the upper layers. The film thickness was 240 nm which allowed us to determine (empiri-

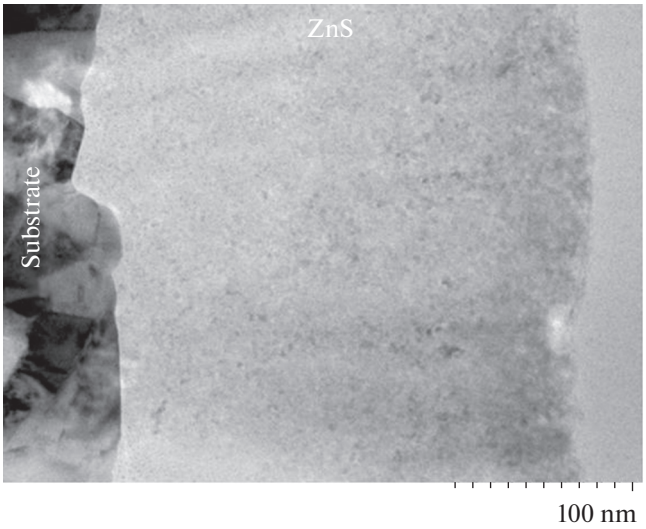

Fig. 3. TEM image of the cross section of a sensor with deposited ZnS film. Deposition conditions: 2.5 mM $ZnSO_4$, 0.04 M Na_2EDTA, 0.2 M thiourea, 1 M NaOH, 65°C.

cally) that the coefficient u is equal to 18.4 ng/(Hz cm^2). Thus, under different deposition conditions the film thickness can be calculated as follows:

$$h = \frac{dm}{S\rho} = \frac{udF}{S\rho} = \frac{18.4\ (\text{ng}/\text{cm}^2)\, dF\ (\text{Hz})}{S\rho} = 0.0453\ \text{nm}/\text{Hz}\ dF, \quad (2)$$

where ρ is the density of zinc sulfide equal to 4.06 g/cm^3, S is the surface of the gold layer on the sensor equal to 1 cm^2.

It deserves mention that the film thickness and the size of deposited particles are close, i.e., the film consists of a monolayer of zinc sulfide particles. At the same time, it cannot be ruled out that the particles immobilized on the sensor will continue to grow or the finer particles remaining in solution will also deposit in the course of long-term reaction and occupy the spaces between deposited particles to form a continuous ZnS layer (Fig. 3).

The Effect of Synthesis Parameters on Characteristics of ZnS Film

The good adhesion and the shorter period before the beginning of film growth corresponded to the following order of bath filling: water, alkali, Na_2EDTA, zinc sulfate, thiourea solution, the holder with the QCM sensor. If this order was disrupted, the induction period could increase several times and the film quality decreased. The induction period decreased and the rate of subsequent growth increased with the increase in the reagent concentration and temperature; moreover, the induction period depended most strongly on these parameters. This also means that the induction period was controlled by the chemical stage, in contrast to film deposition and growth.

The method of gold surface pretreatment was found to substantially affect the deposition process and the film quality. Thus, sulfidization of the surface led to poor adhesion, the treatment with alkali and the presence of organic impurities made the film more porous. The insufficient washing with water after the acid treatment increased the induction period. The etching with the piranha solution turned out to be optimal and we used it in preparation of ZnS films; the results shown in this study correspond to the sensor pretreated in piranha.

Analysis of Deposited Films by Spectroscopic Methods

Figure 4 shows typical XPS spectra of zinc sulfide deposited on the Au surface of sensor. The overview spectra demonstrated lines of zinc and sulfur and also of oxygen and carbon from surface impurities (Fig. 4a). For the thickness of zinc sulfide layer below 180 nm, the lines of gold became visible apparently due to incomplete coverage of the surface by particles. For the thicker films, the spectra showed no gold lines. The intensity ratio of S 2p and Zn 3p lines corresponded to the film with a small excess of sulfur, viz., the atomic ratio Zn/S was equal to 0.85–0.95 for all bath compositions and temperatures. The deficiency of metal on the surface is the general feature associated with sulfide oxidation [20]. The high resolution S 2p and Zn 2p spectra are virtually identical for all samples, containing sufficiently narrow lines and the bonding energy of 161.2 and 1021.6 eV for S $2p_{3/2}$ and Zn $2p_{3/2}$, respectively, which is typical of zinc sulfide. The zinc sulfide particles obtained by evaporation of solution had virtually the identical composition (Fig. 4b); the spectra contained also lines of other solution components (sodium, carbon, nitrogen from thiourea, etc.).

The Raman spectra of films demonstrated no intense peak at 350–360 cm^{-1} due to insufficient crystallinity of the sample; however, the form of spectrum at 240–280 cm^{-1} was characteristic of zinc sulfide in cubic syngony, i.e., sphalerite rather than wurtzite (Fig. 5a). The optical spectrum of particles formed in solution and deposited on glass, which is plotted in the Tauc coordinates, shows (Fig. 5b) that this zinc sulfide has a wide band gap of 3.6 eV, i.e., like sphalerite.

Voltammetric Curves and EQCM Curves

Figure 6a shows the EQCM and CVA curves of a sensor with the ZnS coating in borate solution. In voltammetric curves, the anodic current region corre-

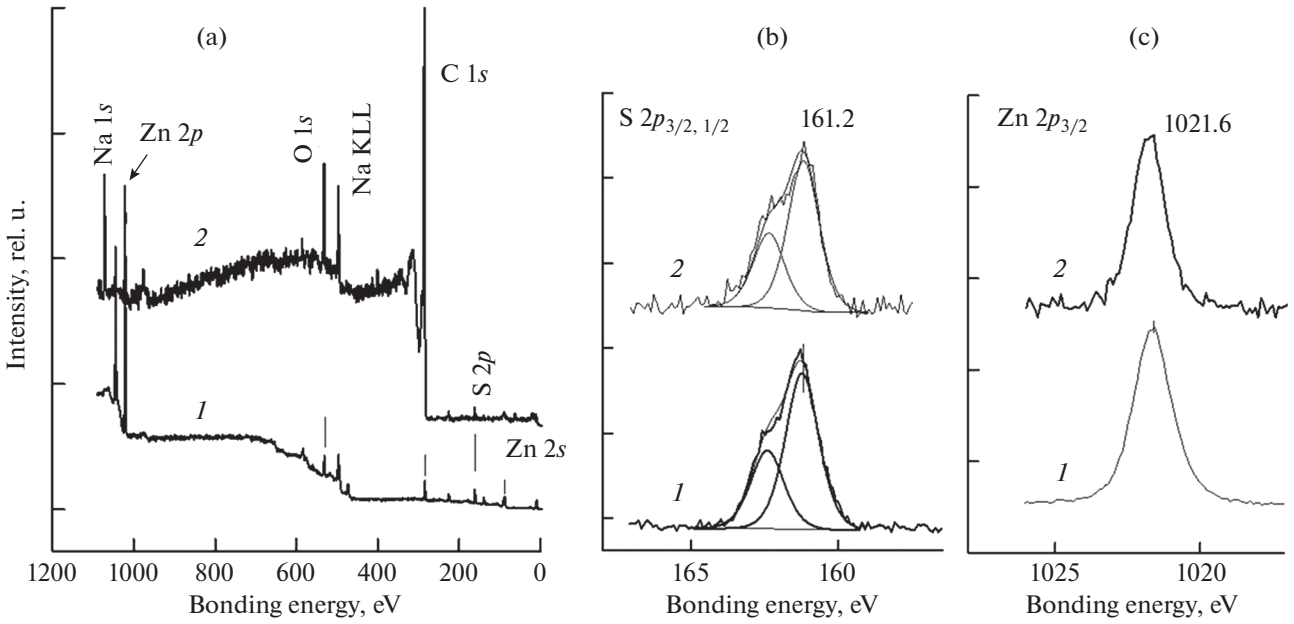

Fig. 4. XPS spectra of (*1*) QCM sensor coated by zinc sulfide film with the thickness of ~230 nm and (*2*) particles formed in solution volume.

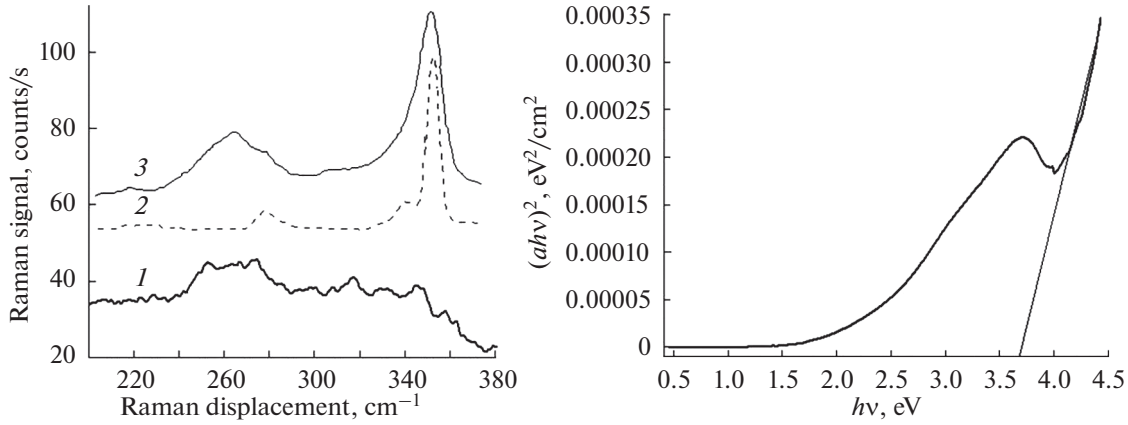

Fig. 5. (a) (*1*) Raman spectrum of ZnS film deposited on the surface of QCM sensor and the literature data for (*2*) wurtzite and (*3*) sphalerite [19]. (b) UV-vis spectrum in Tauc coordinates for zinc sulfide film deposited from a typical bath onto optically transparent glass.

sponds to oxidation and dissolution of zinc sulfide [7, 8] followed by oxygen evolution and gold oxidation [20]. The reverse potential scanning is associated with the gold oxides reduction reflected by the anodic peak K1 [21–23]. These processes were accompanied by the corresponding changes in the sensor frequency. If the anodic potential scan did not proceed beyond 800 mV, the voltammetric curves demonstrated no electrochemical reactions of gold because the zinc sulfide layer was not destroyed to the extent of exposure of the gold surface. Thus, this sensor was stable in this solution in the potential interval from −500 to +800 mV.

In the future, we expect to use the EQCM senor developed here in studying the surface phenomena and processes occurring under the conditions of flotation where potassium butylxanthate is widely used as the collector. In the pilot experiments with addition of the latter substance into the working solution, an anodic shoulder appeared starting from 100 mV (Fig. 6b) which corresponded to oxidation of adsorbed xanthate ions; in this case the process rate was limited by diffusion. The decrease in the sensor frequency in the anodic region was probably associated with the adsorption of butylxanthate and dixanthate formed at oxidation. The decrease in the sensor frequency was

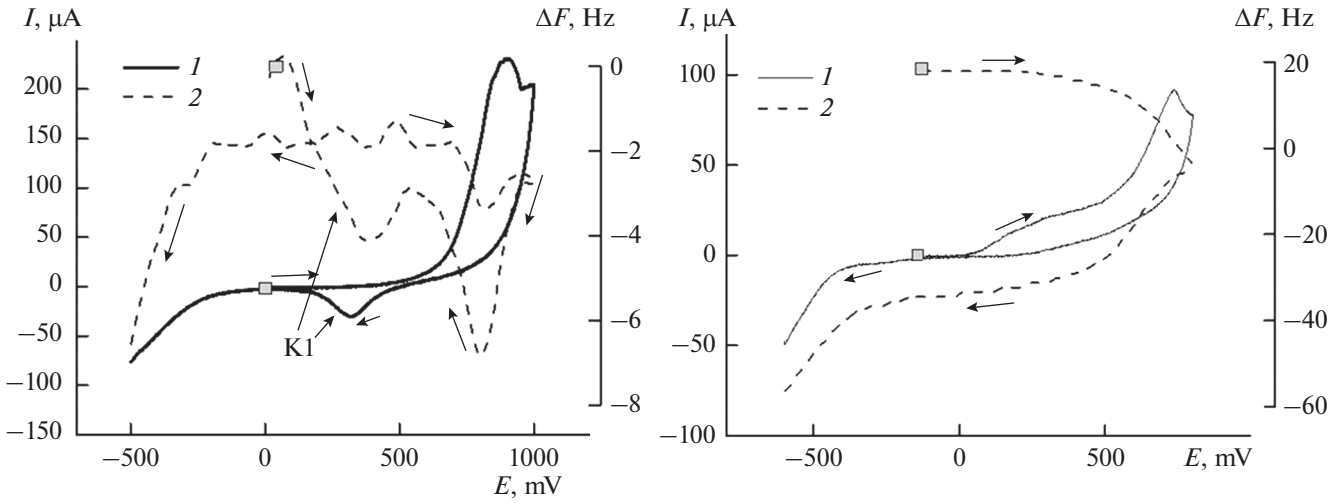

Fig. 6. (*1*) CVA curves and (*2*) the dependences of the frequency of quartz sensor vibrations in (a) 0.05 M borate buffer and (b) 0.05 M borate buffer + 5×10^{-5} potassium butylxanthate. Electrode surface—gold sputtered onto quartz and covered by a zinc sulfide layer.

probably caused by the adsorption of H_3O^+ ions. These processes require more detailed study and are beyond the scope of our study.

CONCLUSIONS

The conditions are found for the preliminary treatment of the gold surface and the formation of a thin uniform sphalerite film on its surface to obtain a senor with the ZnS coating. The efficiency of this sensor is demonstrated by the methods of EQCM and cyclic voltammetry (CVA). The surface treatment procedure is observed to affect the adhesion and the quality of coating. It is shown that the best adhesion and uniformity of the coating corresponds to the QCM sensor is etched in the piranha solution. The presence of sulfide sulfur and traces of hydrocarbons on the surface before the deposition prevents the uniform and dense adhesion. The DLS and QCM studies have shown that the deposition of zinc sulfide particles on the sensor surface starts in the moment of the loss of colloidal stability of particles formed in the liquid phase. The studies by the methods of XPS and Raman and optical spectroscopy have shown that the synthesized zinc sulfate is sphalerite with the forbidden zone of 3.6 eV.

FUNDING

The study was supported by the Russian Scientific Foundation (grant no. 18-17-00135.

CONFLICT OF INTERESTS

The authors declare that there is no conflict of interest.

REFERENCES

1. Tyrakowski, C.M. and Snee, P.T., Ratiometric CdSe/ZnS quantum dot protein sensor, *Anal. Chem.*, 2014, vol. 86, p. 2380.
2. Dehghani, Z., Nazerdeylami, S., Saievar-Iranizad, E., and Majles Ara, M.H., Synthesis and investigation of nonlinear optical properties of semiconductor ZnS nanoparticles, *J. Phys. Chem. Solids.*, 2011, vol. 2, p. 1008.
3. Borah, J.P. and Sarma, K.C., Optical and optoelectronic properties of ZnS nanostructured thin film, *Acta Phys. Pol., A*, 2008, no. 4, vol. 114, p. 713.
4. Ke, W., Stoumpos, C.C., Logsdon, J.L., Wasielewski, M.R., Yan, Y., Fang, G., and Kanatzidis M.G., TiO_2–ZnS cascade electron transport layer for efficient formamidinium tin iodide perovskite solar cells, *J. Am. Chem. Soc.*, 2016, vol. 138, p. 14998.
5. Mikhlin, Y., Karacharov, A., Vorobyev, S., Romanchenko, A., Likhatski, M., Antsiferova, S., and Markosyan, S., Towards understanding the role of surface gas nanostructures: Effect of temperature difference pretreatment on wetting and flotation of sulfide minerals and Pb–Zn ore, *Nanomaterials*, 2020, vol. 10, p. 1362.
6. Mikhlin, Yu., Karacharov, A., Tomashevich, Ye., and Shchukarev, A., Interaction of sphalerite with potassium *n*-butyl xanthate and copper sulfate solutions studied by XPS of fast-frozen samples and zeta-potential measurement, *Vacuum*, 2016, vol. 125, p. 98.
7. Ahlberg, E. and Asbjornsson J., Carbon paste electrodes in mineral processing: an electrochemical study of sphalerite, *Hydrometallurgy*, 1994, vol. 36, p. 19.
8. Zhuo, C. and Roe-Hoan, Y., Electrochemistry of copper activation of sphalerite at pH 9.2, *Int. J. Miner. Process.*, 2000, vol. 58, p. 57.
9. Teng, F., Liu, Q., and Zeng, H., In situ kinetic study of zinc sulfide activation using a quartz crystal microbal-

ance with dissipation (QCM-D), *J. Colloid Interface Sci.*, 2012, vol. 368, no. 1, p. 512.

10. O'Brien, P. and McAleese, J., Developing an understanding of the processes controlling the chemical bath deposition of ZnS and CdS, *J. Mater. Chem.*, 1998, vol. 8, no. 11, p. 2309.
11. Doña, J.M., Process and film characterization of chemical-bath-deposited ZnS thin films, *J. Electrochem. Soc.*, 1994, vol. 141, no. 1, p. 205.
12. Hodes, G., *Chemical solution deposition of semiconductor films*, New York: Marcel Dekker, 2002.
13. Agawane, G.L., Kim, S.S., Sung, M., Suryawanshi, M.P., Gurav, K.V., Moholkar, A.V., Lee, J. Y., Ho, Y.J., Patil, P.S., and Hyeok, K.J., Green route fast synthesis and characterization of chemical bath deposited nanocrystalline ZnS buffer layers, *Curr. Appl. Phys.*, 2003, vol. 13, no. 5, p. 850.
14. Akhtar, M.S., Malik, M.A., Riaz, S., Naseem, S., and O'Brien, P., Optimising conditions for the growth of nanocrystalline ZnS thin films from acidic chemical baths, *Mater. Sci. Semicond. Process.*, 2015, vol. 30, p. 292.
15. Bayer, A., Boyle, D.S., and O'Brien, P., In situ kinetic studies of the chemical bath deposition of zinc sulfide from acidic solutions, 2002, *J. Mater. Chem.*, 2002, vol. 12, p. 2940.
16. Sauerbrey, G., Verwendung von schwingquarzen zur wägung dünner schichten und zur mikrowägung, *Z. Phys.,* 1959, vol. 55, no. 2, p. 206.
17. Hinsberg, W.D., Willson, C.G., and Kanazawa, K.K., Measurement of thin-film dissolution kinetics using a quartz crystal microbalance, *J. Electrochem. Soc.*, 1986, p. 1448.
18. Mengsu, Y., Thompson, M., and Duncan-Hewitt, W.C., Interfacial properties and the response of the thickness-shear-mode acoustic wave sensor in liquids, *Langmuir*, 1993, vol. 9, no. 3, p. 802.
19. Cheng, Y.C., Jin, C.Q., and Gao, F., Raman scattering study of zinc blende and wurtzite ZnS, *J. Appl. Phys.*, 2009, vol. 106, p. 123505.
20. Mikhlin, Y., X-ray photoelectron spectroscopy in mineral processing studies, *Appl. Sci.,* 2020, vol. 10, p. 5138.
21. Doyle, R.L. and Lyons, M.E.G., The mechanism of oxygen evolution at superactivated gold electrodes in aqueous alkaline solution, *J. Solid State Electrochem.*, 2014, vol. 18, p. 3271.
22. Adžić, R.R., Strbac, S., and Anastasijević, N., Electrocatalysis of oxygen on single crystal gold electrodes, *Mater. Chem. Phys.*, 1989, vol. 22, no. 3–4, p. 349.
23. Burke, L.D., Ahern, A.J., and O'Mullane, A.P., High energy states of gold and their importance in electrocatalytic processes at surfaces and interfaces, *Gold Bull.*, 2002, vol. 35/1, p. 3.

Translated by T. Safonova